

Supporting information

A Visual Logic Alarm Sensor for Diabetic Patients towards Diabetic Polyneuropathy Based on Metal-Organic Framework Functionalized by Dual-Cation Exchange

Yu Zhang^{‡^a}, Xianglong Qu^{‡^a} and Bing Yan^{*^{a, b}}

*^a School of Chemical Science and Engineering, Tongji University, 1239 Siping Road, Shanghai
200092, China*

^b School of Materials Science and Engineering, Liaocheng University, Liaocheng 252059, China

Corresponding author Email addresses: byan@tongji.edu.cn (Bing Yan)

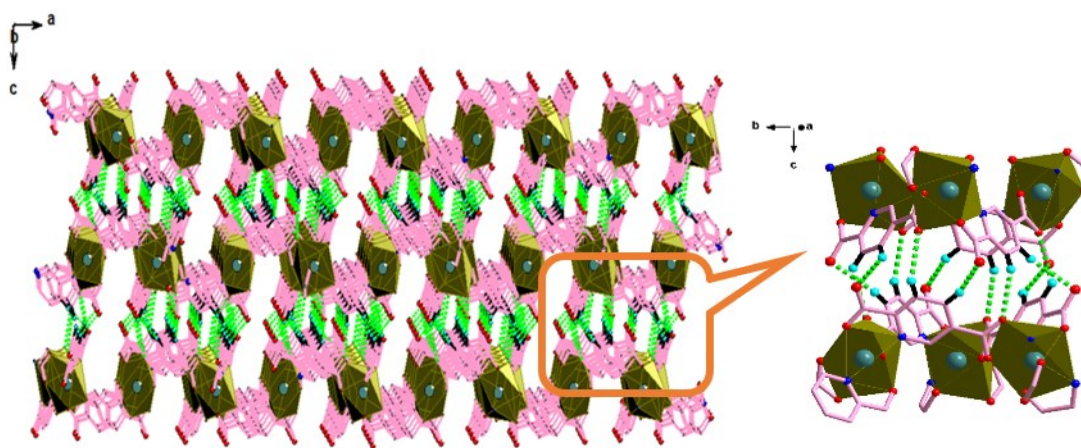


Figure S1 Packing view of the In-pdc layers stacked along c direction based on C4–H4···O4 and C5–H5···O2 hydrogen bonds.

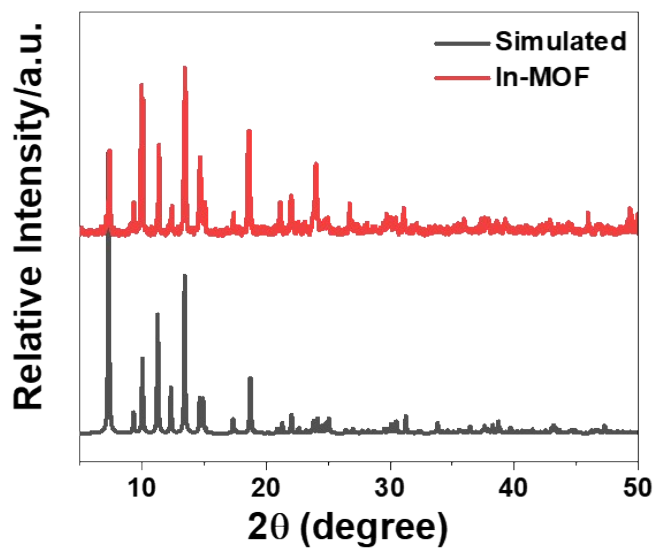


Figure S2 The PXRD patterns of In-MOF and simulated one.

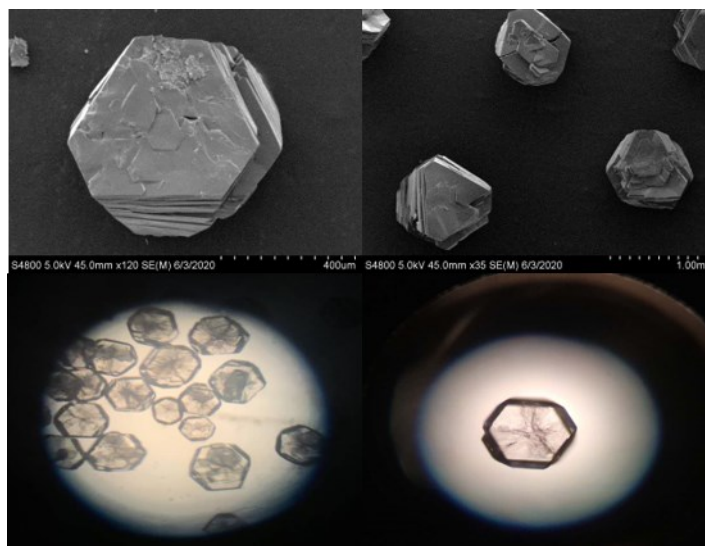


Figure S3 The SEM image and optical images of In-MOF.

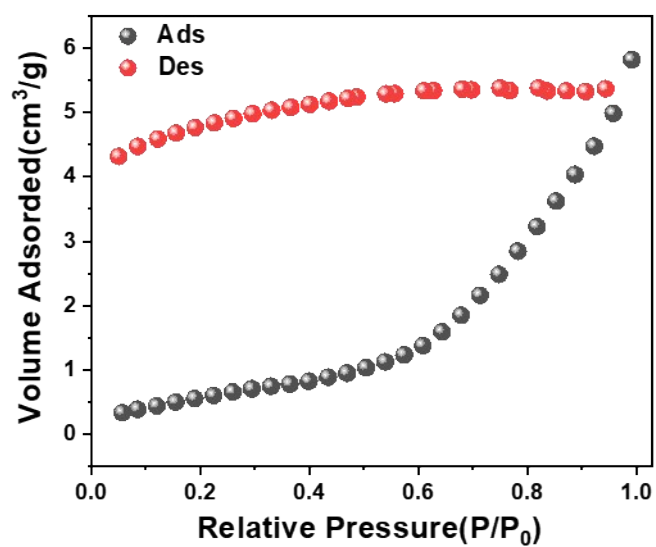


Figure S4 N₂ adsorption/desorption isotherms of In-MOF.

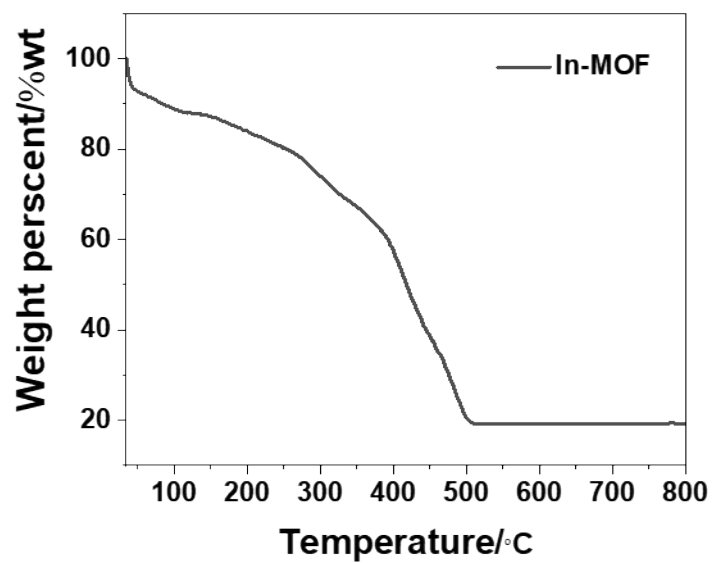


Figure S55 Thermal gravimetric analysis curves for In-MOF.

1

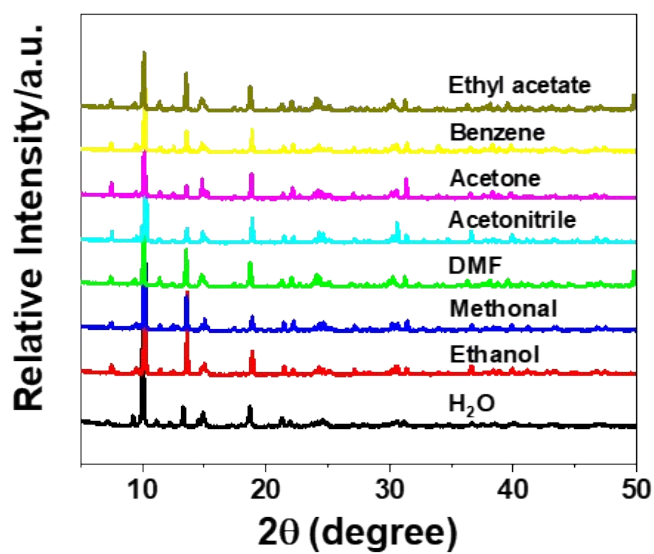


Figure S6 PXRD of In-MOF after being immersed in common solvents.

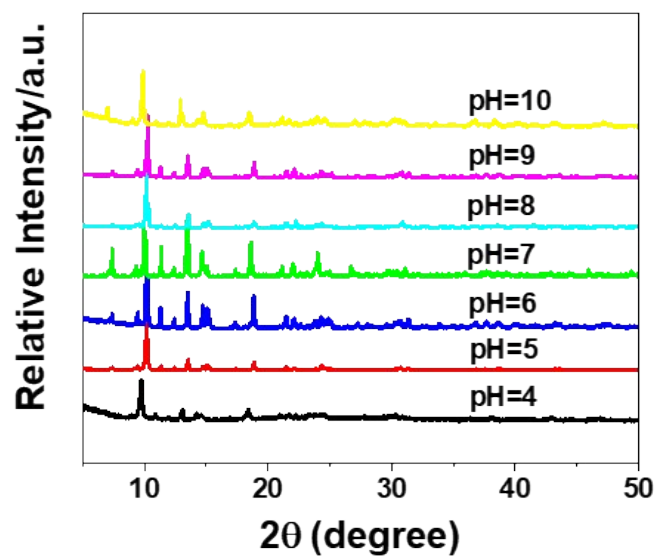


Figure S7 PXR D of In-MOF after being immersed in the solutions of pH = 4-10.

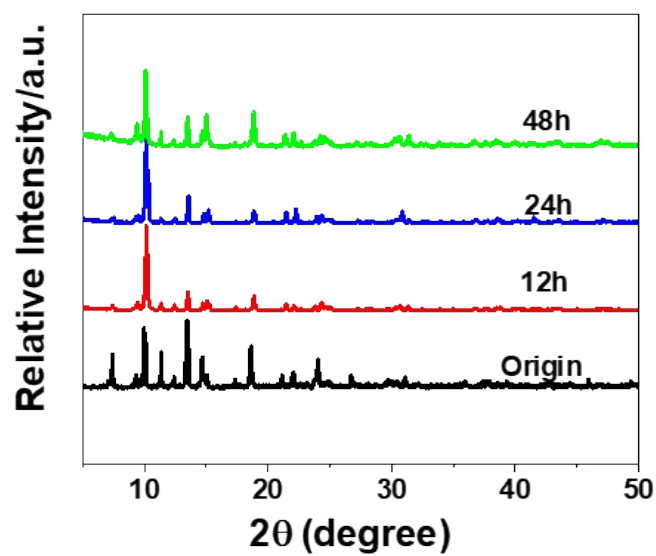


Figure S8 PXR D of In-MOF after being immersed in the H_2O for 12-48h.

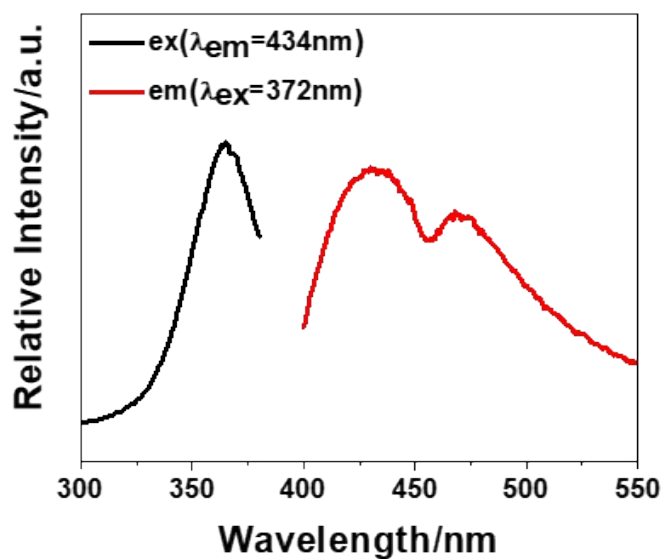


Figure S9 Excitation (black line) and emission (red line) spectra of H₂pdc.

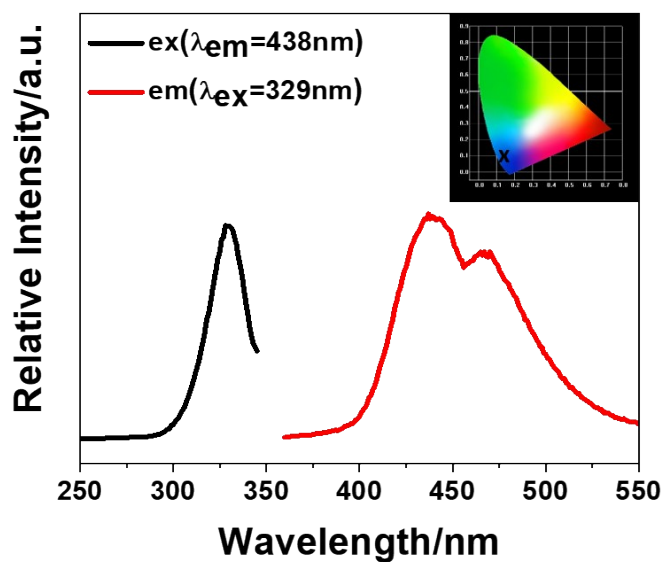


Figure S10 Excitation (black line) and emission (red line) spectra of In-MOF (The inset is the corresponding CIE chromaticity diagram of In-MOF).

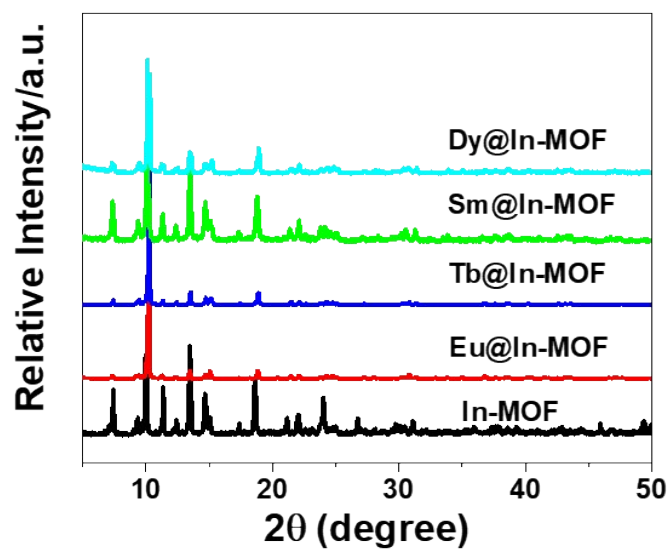


Figure S11 PXRD of Eu@In-MOF, Tb@In-MOF, Sm@In-MOF and Dy@In-MOF.

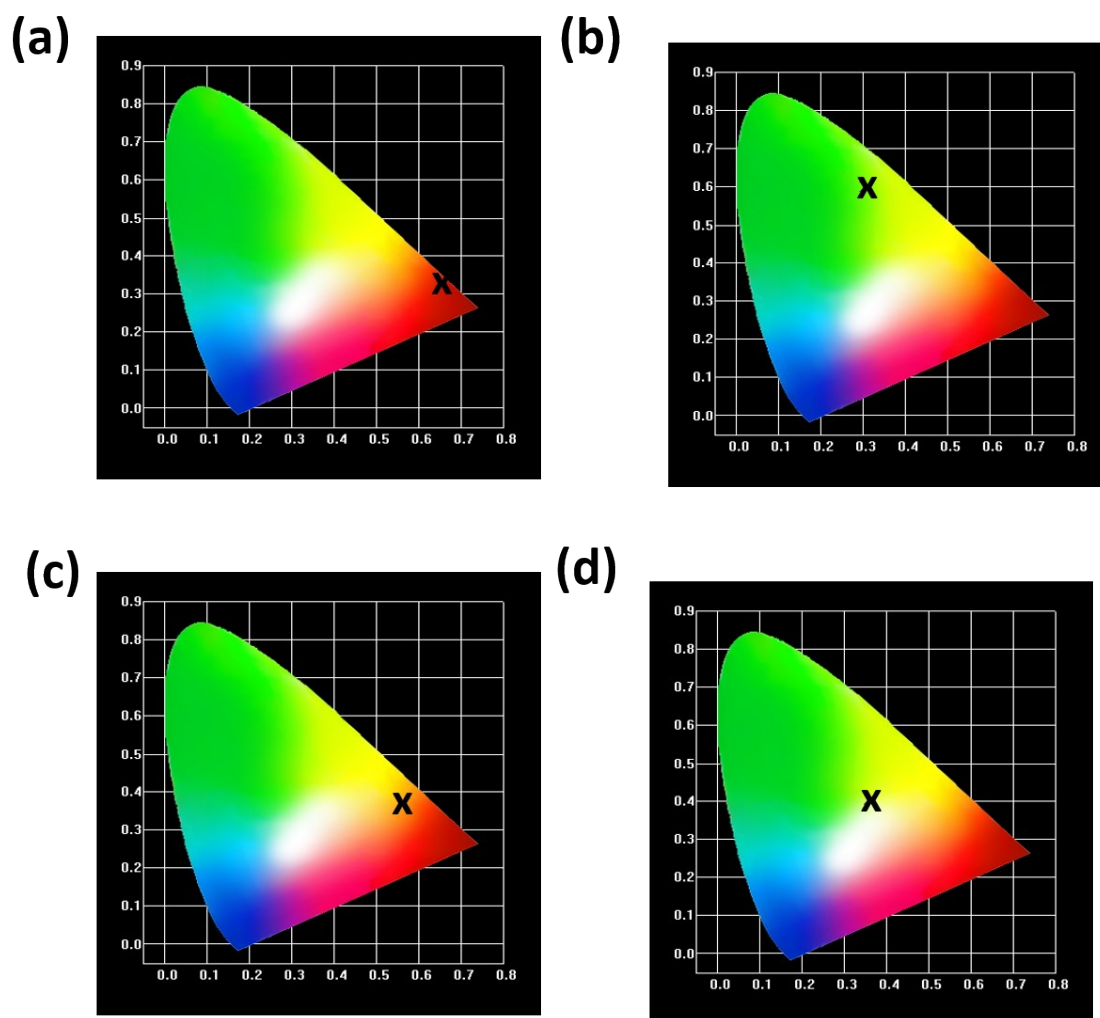


Figure S12 Corresponding CIE chromaticity diagram of (a) Eu@In-MOF; (b) Tb@In-MOF (c) Sm@In-

MOF; (d) Dy@In-MOF.

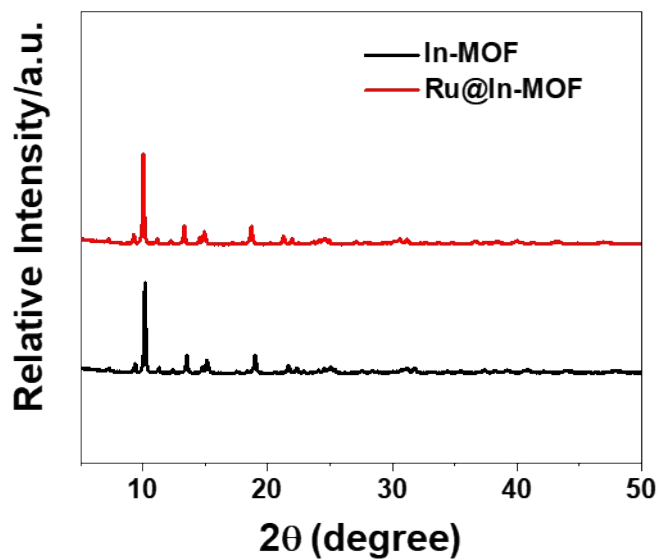


Figure S13 PXRD of In-MOF and Ru@In-MOF.

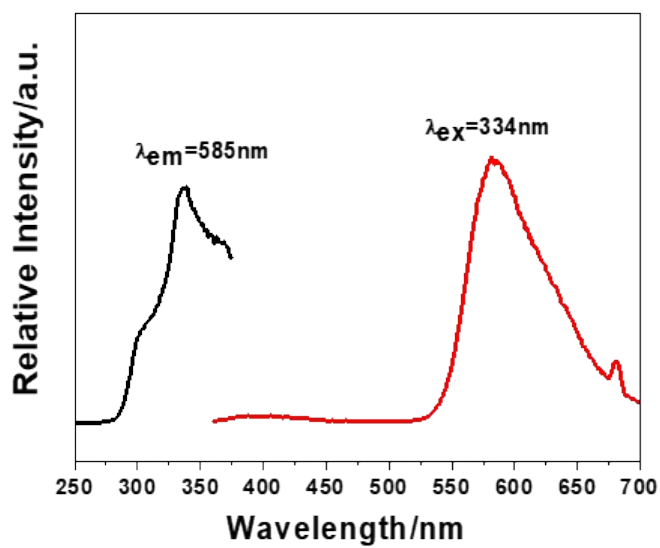


Figure S14 Excitation (black line) and emission (red line) spectra of Ru@In-MOF.

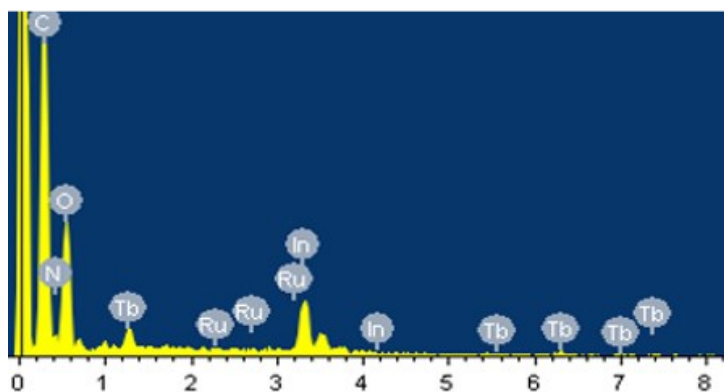


Figure S15 Energy dispersive analysis by X-rays (EDX) spectroscopy of **Ru/Tb@In-MOF**.

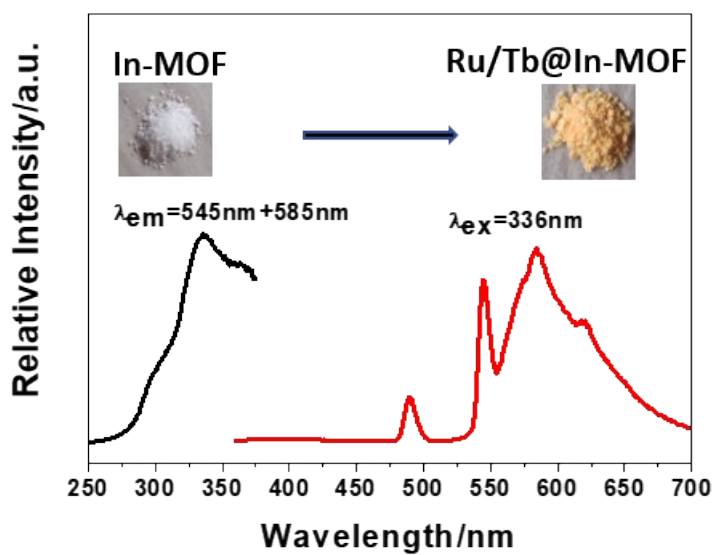


Figure S16 Excitation (black line) and emission (red line) spectra of **Ru/Tb@In-MOF** (The inset is the photo of In-MOF and Ru/Tb@In-MOF power).

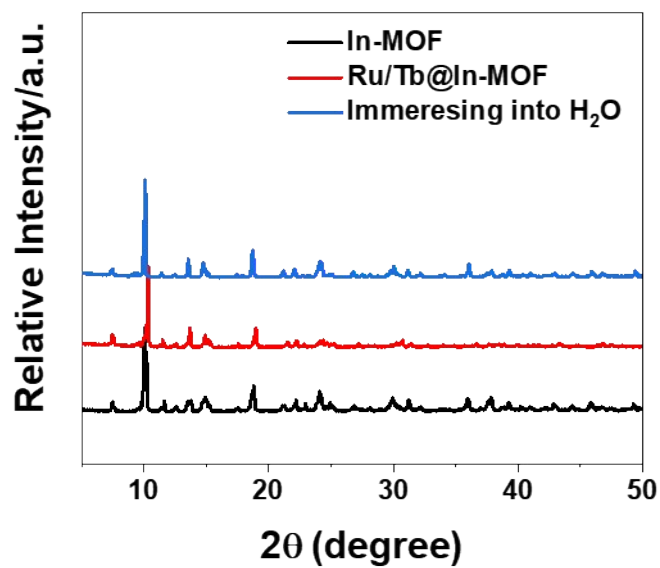


Figure S17 PXRD patterns of In-MOF, Ru/Tb@In-MOF and Ru/Tb@In-MOF immersing into H₂O.

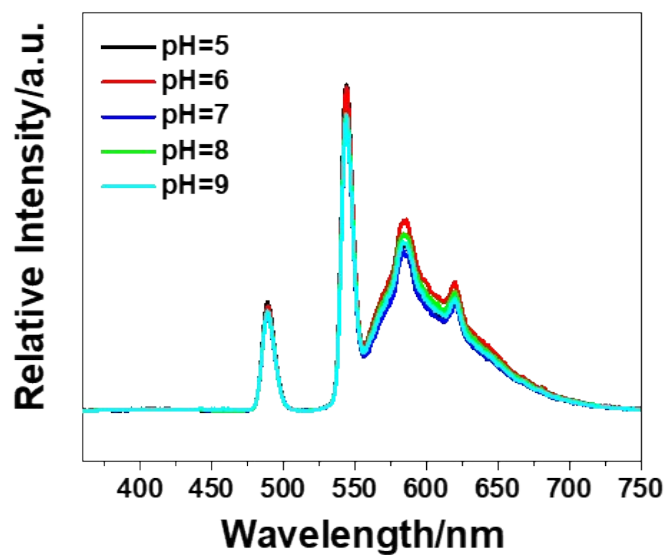


Figure S18 Emission spectra of Ru/Tb@In-MOF in different pH solutions.

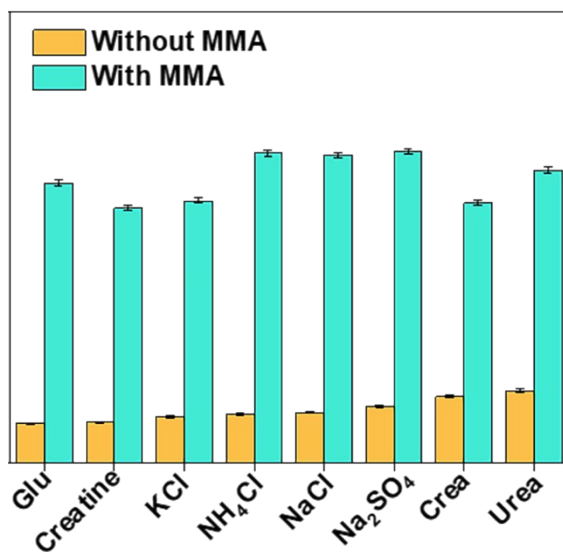
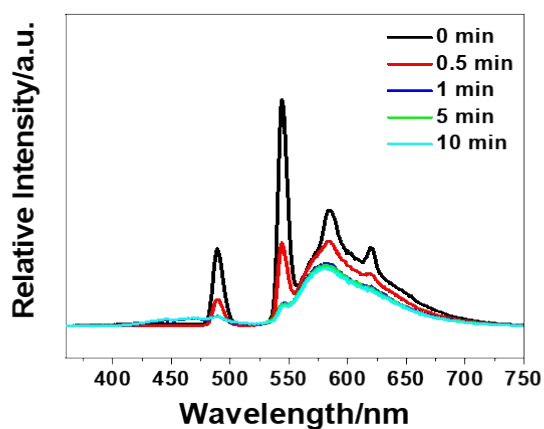


Figure S19 Luminescence responses of **Ru/Tb@In-MOF** ($I_{585\text{nm}}/I_{545\text{nm}}$) toward other urine components with and without MMA.

(a)



(b)

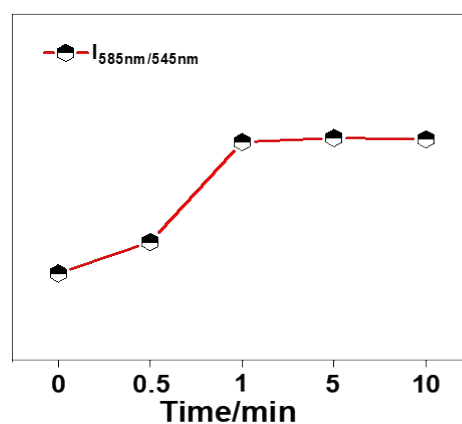


Figure S20 (a) Variation of luminescent intensity of **Ru/Tb@In-MOF** with different immersion time in MMA; (b) The corresponding line chart.

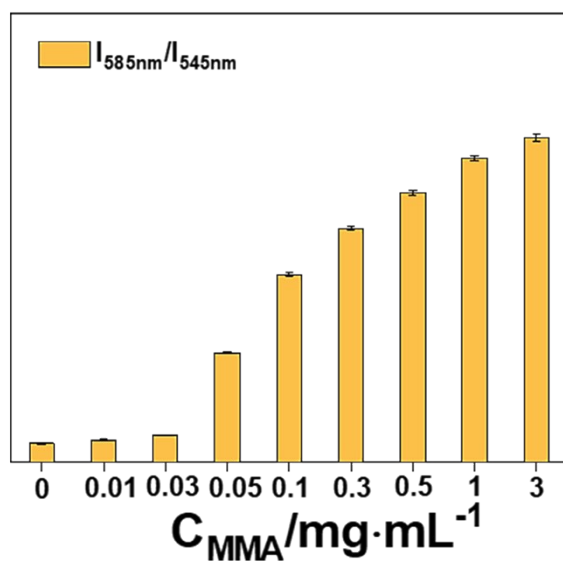


Figure S21 The column diagram of the fluorescence intensity of Ru/Tb@In-MOF ($I_{585\text{nm}}/I_{545\text{nm}}$) after immersing into different concentrations of MMA.

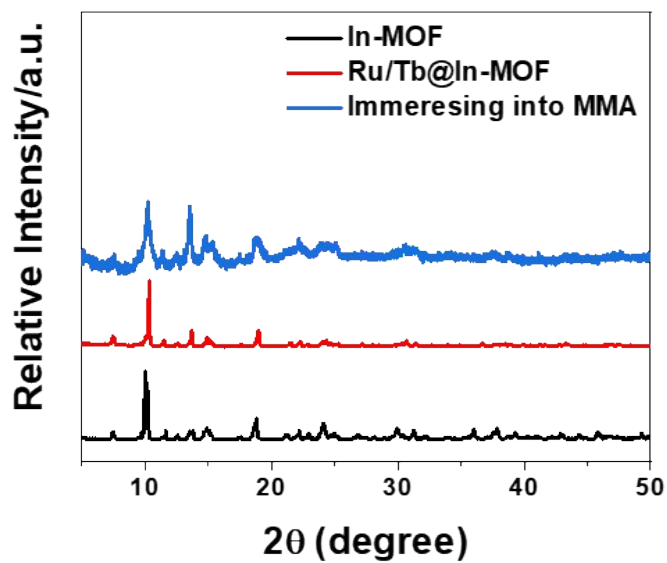


Figure S22 PXRD patterns of In-MOF, Ru/Tb@In-MOF and Ru/Tb@In-MOF immersing into MMA.

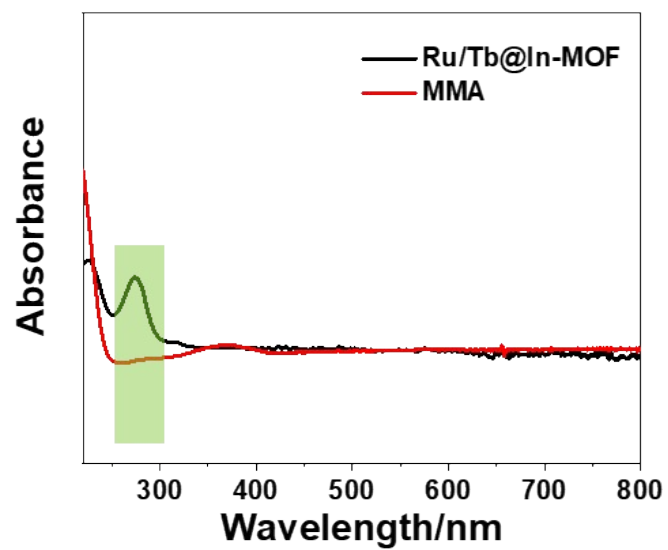


Figure S23 UV-vis spectra of Ru/Tb@In-MOF and MMA.

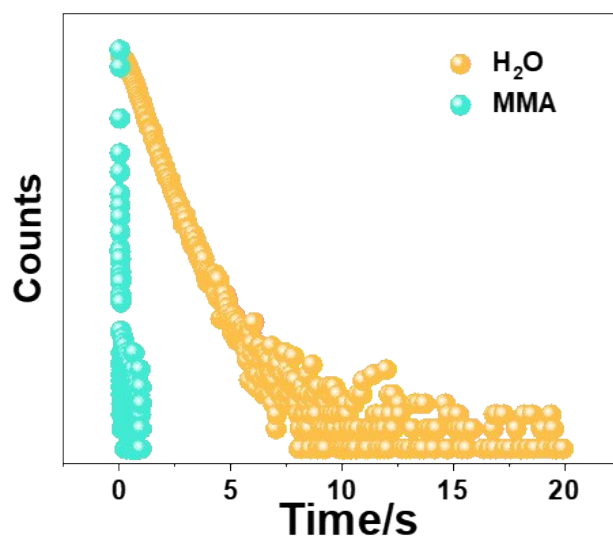


Figure S24 Luminescence decay curves of Ru/Tb@In-MOF immersed in H₂O and MMA.

Table S1 Crystal data and structure refinement for **In-MOF**

Complex	In-MOF
Empirical formula	C ₁₆ H ₁₄ N ₃ O ₈ In
Formula weight	491.03
monoclinic	
Space group	R-3c
<i>a</i> / Å	15.7001(4)
<i>b</i> / Å	15.7001(4)
<i>c</i> / Å	52.849(3)
α / (°)	90
β / (°)	90
γ / (°)	120
Volume / Å ³	11281.6(8)
<i>Z</i>	18
Calculated density / mg·m ⁻³	1.179
Absorption coefficient / mm ⁻¹	0.972
<i>F</i> (000)	3906
Crystal size / mm	0.36 × 0.24 × 0.12
θ Range for data collection / (°)	3.09-27.573
	-20 ≤ <i>h</i> ≤ 20
Limiting indices	-20 ≤ <i>k</i> ≤ 20
	-68 ≤ <i>l</i> ≤ 67
	50685/2905
Reflections collected / unique	[<i>R</i> (int)=0.0625]
Data / restraints / parameters	2905/0/114
Goodness-of-fit on <i>F</i> ²	1.050
<i>R</i> ₁ [<i>I</i> > 2σ(<i>I</i>)]	0.0518
w <i>R</i> ₂ [<i>I</i> > 2σ(<i>I</i>)]	0.1904
<i>R</i> ₁ [all data]	0.0650
w <i>R</i> ₂ [all data]	0.2005
Largest diff. peak and hole / e·Å ⁻³	2.291 and -0.800
CCDC	2023759

Table S2 Selected bond lengths [Å] for In-MOF

In-MOF	
In(1)-O(1)#1	2.157(4)
In(1)-O(1)	2.157(4)
In(1)-O(3)#2	2.199(4)
In(1)-O(3)#3	2.199(4)
In(1)-N(1)#2	2.269(4)
In(1)-N(1)#3	2.269(4)
O(1)#1-In(1)-O(1)	95.0(2)
O(1)-In(1)-O(3)#3	83.75(16)
O(1)-In(1)-O(3)#2	125.08(15)
O(1)#1-In(1)-O(3)#3	125.07(15)
O(1)#1-In(1)-O(3)#2	83.75(16)
O(1)#1-In(1)-N(1)#3	86.30(16)
O(1)-In(1)-N(1)#2	86.31(16)
O(1)-In(1)-N(1)#3	152.07(16)
O(1)#1-In(1)-N(1)#2	152.08(16)
O(3)#3-In(1)-O(3)#2	139.6(2)
O(3)#2-In(1)-N(1)#2	72.93(14)
O(3)#2-In(1)-N(1)#3	82.82(15)
O(3)#3-In(1)-N(1)#3	72.94(14)
O(3)#3-In(1)-N(1)#2	82.83(15)
N(1)#3-In(1)-N(1)#2	105.3(2)

Symmetry transformations used to generate equivalent atoms: #1 $-x+4/3, -x+y+2/3, -z+7/6$; #2 $-y+1, x-y+1, z$; #3 $y+1/3, x+2/3, -z+7/6$.

Table S3 Repeated ICP-MS results of Ru/Tb@In-MOF.

Ru/Tb@TJU-12	Content of In	Content of Tb	Content of Ru
1	14.96%	5.27%	3.26%
2	15.15%	4.91%	3.57%
3	14.68%	5.05%	3.06%

Table S4 The luminescence decay times of Ru/Tb@In-MOF in H₂O and MMA.

Substance	Lifetimes(μs)
H₂O	858.53μs
MMA	10.31μs